ACS APPLIED MATERIALS & INTERFACES

Research Article

www.acsami.org

Highly Reproducible and Sensitive SERS Substrates with Ag Inter-Nanoparticle Gaps of 5 nm Fabricated by Ultrathin Aluminum Mask Technique

Qun Fu,[†] Zhibing Zhan,[‡] Jinxia Dou,[†] Xianzheng Zheng,[†] Rui Xu,[‡] Minghong Wu,*[,†] and Yong Lei*[,†,‡]

[†]Institute of Nanochemistry and Nanobiology, School of Environmental and Chemical Engineering, Shanghai University, Shanghai 200444, P. R. China

[‡]Institute for Physics and IMN MacroNano (ZIK), Technical University of Ilmenau, Prof. Schmidt Straße 26, 98693 Ilmenau, Germany

Supporting Information

ABSTRACT: Applicable surface enhanced Raman scattering (SERS) active substrates require high enhancement factor (EF), excellent spatial reproducibility, and low-cost fabrication method on a large area. Although several SERS substrates with high EF and relative standard deviation (RSD) of signal less than 5% were reported, reliable fabrication for large area SERS substrates with both high sensitivity and high reproducibility via low-cost routes remains a challenge. Here, we report a facile and cost-effective fabrication process for large-scale SERS substrate with Ag inter-nanoparticle (NP) gaps of 5 nm based on ultrathin alumina mask (UTAM) surface pattern technique. Such closely packed Ag NP arrays with high density of electromagnetic field enhancement ("hot spots") on large area exhibit high SERS activity and excellent reproducibility, simultaneously. Rhodamine 6G molecules with concentration of 1×10^{-7} M are used to determine the SERS performance, and an EF of $\sim 10^9$ is obtained. It should be noted that we obtain RSDs about 2% from 10 random spots on an area of 1 cm^2, which implies the highly reproducible signals. Finite-difference time-domain simulations further suggest that the enhanced electric field originates from the narrow gap, which agrees well with the experimental results. The low value of RSD and the high EF of SERS signals indicate that the as-prepared substrate may be promising for highly sensitive and uniform SERS detection.

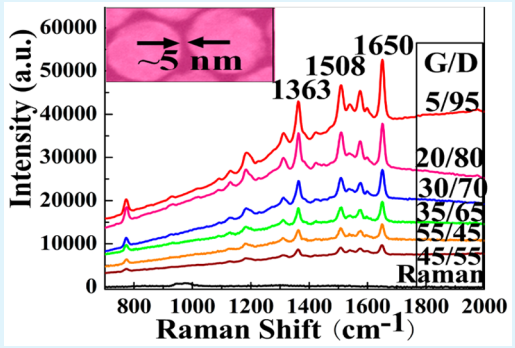

KEYWORDS: *SERS, Ag nanoparticles, ultrathin alumina mask technique, nanogaps of 5 nm, high reproducibility*

1. INTRODUCTION

Surface enhanced Raman scattering (SERS) spectroscopy has been considered one of the most powerful probing tools in ultrasensitive analysis[1,2] since its discovery in 1974[3] and 1977,[4] due to the tremendous enhancement for the normally weak Raman signal of analytes. The enhancement of Raman signals is primarily attributed to the electromagnetic (EM) field induced by the localized surface plasmon resonance (LSPR) on the surface of noble metals. Large EM field enhancement occurs at specific sites, also called "hot spots",[5] which usually locate at the gaps between the two adjacent coupling metal nanoparticles (NPs) with distance on the order of a few nanometers.

Applicable SERS substrates require high enhancement factor (EF), excellent spatial reproducibility,[6−8] and fabrication on large area through a cost-effective method. In order to obtain high EF and excellent reproducibility, hot spots with small size, high density and homogeneity in distribution are crucial for SERS substrates.[5,9−11] Various methods have focused on the fabrication of SERS substrates with sub-10-nm gaps. Clustering[11−14] of chemically synthesized NPs can get remarkable SERS enhancement, but its poor reproducibility hinders the further application of SERS. Lithographic methods, such as electron-beam lithography,[13,15−17] nanosphere lithography,[18] focused ion-beam patterning,[19] and soft lithography[20,21] are commonly used to produce tightly spaced plasmonic geometries. However, highly specialized lithographic facilities are complex and expensive, and tedious preparation and implementation steps (lithography and lift-off) require accuracy and time consumption.[22] Other methods also have limitations to fabricate high-quality SERS substrates with high reproducibility and a large number of hot spots (e.g., electromigration is difficult to prepare nanostructures on large area,[23,24] physical vapor deposition itself can not fabricate nanostructure arrays, chemical vapor deposition and atomic layer deposition are only applicable to limited classes of materials,[25,26] and on-wire lithography can only handle nanowires[27−31]). Template technique is regarded as one of the unique fabrication methods for well-ordered periodic nanostructures on large area.[32−34] In

Received: February 16, 2015
Accepted: May 29, 2015
Published: May 29, 2015

DOI: 10.1021/acsami.5b01524
ACS Appl. Mater. Interfaces 2015, 7, 13322−13328

recent works,[35−39] ultrathin alumina mask (UTAM) surface nanopatterning technique has already shown many advantages, such as easy fabrication on a large scale (>1 cm^2), size controllability, excellent regularity and reproducibility, ultrahigh density (10^{10}−10^{12} cm^{-2}) of nanostructures, and low equipment costs. Several works reported SERS substrates with nanoarrays templated by anodized aluminum oxide (AAO).[5,9,40−43] However, these ordered nanostructure arrays either show good enhancement but poor uniformity because of the thick template with deep channel, or show high reproducibility but normal EF due to their large nanostructure separation. It has also been reported that SERS spectra on the current metal−AAO SERS substrates have rather strong luminescence background which would interfere with SERS signals tremendously.[44] Although high EF can be achieved and several SERS substrates with signal relative standard deviation (RSD) value less than 5% were reported,[9,42,45] reliable fabrication of large area SERS substrates with both high sensitivity and high reproducibility through a low-cost route remains a challenge, because it is rather difficult to achieve reproducible "hot spots" with ultrasmall size, high density, and homogeneous distribution over the entire area of the SERS substrate.

On the basis of a UTAM surface pattern technique, we report here a convenient method to fabricate hot-spot-active SERS substrates with Ag interparticle gaps as small as 5 nm on large area. Rhodamine 6G (R6G) with concentration of 1×10^{-7} M was used to determine the SERS performance, and an EF of $\sim 10^9$ was obtained. It is noteworthy that we obtained RSDs of about 2% from 10 random spots on an area of 1 cm^2, which implies highly reproducible signals. To our knowledge, this reproducibility with high SERS enhancement in such a large area is the best in the reported SERS substrates. It should be noted that, because of the resonant effect of the R6G under the illumination of 514.5 nm, the molecule signals observed in all experiments were surface enhanced resonance Raman scattering (SERRS)[46] but will be referred to as SERS for simplicity.[47] Finite-difference time-domain (FDTD) simulations further suggest that the enhanced electric field originated from the narrow gap, which agrees well with the experimental results. This easy and effective fabrication method could be used for label-free immunoassays, biosensing, and environmental monitoring and detecting.

2. EXPERIMENTAL SECTION

Fabrication of UTAMs. The UTAMs were prepared using a two-step anodization process.[35−39,48] In brief, after a series of pretreatments the high-purity (99.999%) aluminum foil with 0.2 mm thickness was first anodized in 0.3 M oxalic acid aqueous solution at 10 °C and 40 V dc for 12 h. Then, the anodic oxide layer was removed in a mixture of H_3PO_4 (6 wt %) and H_2CrO_4 (1.8 wt %) at 60 °C. Secondary anodization was carried out using the same condition as the first step for 5 min, and then the Al layer was removed in a $CuCl_2$/HCl solution. After that, the pore-widening process was carried out in 5 wt % phosphoric at 30 °C for 45−75 min for different samples, and the UTAMs with various pore sizes were obtained by adjusting the pore-widening time. Finally, as-prepared UTAMs were attached on the Si substrate for use. More details are shown in Supporting Information.

Preparation of Active Substrates with Ordered Ag Nanoparticle Arrays. Ag was thermally evaporated on the UTAM/Si substrate under the vacuum of 8.4×10^{-4} Pa with an evaporation rate of 0.4 nm s^{-1}. The distance between the sample and the evaporation source was 11 cm. After deposition of 50-nm-thick Ag (the thickness was measured by the crystal thickness monitor of the evaporator, i.e., nominal layer thickness), UTAMs were stripped away, leaving the ordered Ag NP arrays on the surface of the substrate. By changing the UTAM structure parameters, a series of Ag NPs arrays with different diameter and particle separation were achieved. More details are shown in Supporting Information.

Preparation of Samples for SERS Measurement. The samples for SERS measurements were prepared by immersion of the substrates in identical 10^{-7} M R6G aqueous solution (30 mL) for 3 h to make sure the surface especially the "hot spots" adsorbed a layer of R6G molecules. To determine the EFs, a bare Si substrate without Ag deposition was immersed in 0.2 M R6G aqueous solution for 3 h as the controlling. For comparison, ordinary 50 nm-thick Ag film substrate was immersed in 10^{-7} M R6G aqueous solution for 3 h to measure its SERS signal. Subsequently, all the samples were rinsed with deionized water and dried by nitrogen gas flow.

Characterization and SERS Measurement. Scanning electron microscopy (SEM) images were obtained on an FE-SEM (JSM-6700 F, JEOL) with an energy dispersion X-ray spectrometer (EDS, JEOL Company). SERS spectra were collected by a 100× N.A. 0.9 objective Renishaw System 1000 Raman spectrometer with 514.5 nm wavelength argon ion laser excitation in cumulative exposure time of 50 s, and the laser power density was adjusted to about 2.62×10^9 mW/cm^2. All the SERS spectra were acquired from 5 to 6 different locations of the same sample, and the typical spectrum was reported. Baseline correction of the measured spectra was performed to remove the broad background and fluorescence band. All the experiments were performed in duplicate or triplicate to check the repeatability of the whole process.

3. RESULTS AND DISCUSSION

Figure 1 schematically outlines the procedure for fabricating Ag NP array SERS-active substrate with tunable diameters (D) and

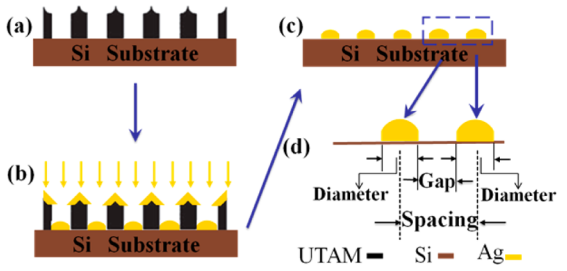

Figure 1. Schematic illustration of the process for fabricating Ag NP array SERS-active substrate with UTAM as template: (a) UTAM transferred onto Si substrate, (b) deposition of Ag by evaporation with UTAM as shadow mask, (c) Ag NP arrays after UTAM removing, and (d) two amplificatory adjacent Ag NPs with certain diameter, gap, and spacing.

gaps (G) using UTAM as a template. First, the prepared UTAM was transferred onto a silicon substrate (Figure 1a), and then Ag NPs were deposited on the Si substrate by thermal evaporation in the vacuum condition using UTAM as shadow mask (Figure 1b). After UTAMs are removed, the regular Ag NP arrays with tunable diameter and interparticle gaps are obtained on the surface of the Si substrate (Figure 1c,d). For fabrication of UTAM, the spacing size (or cell size, center to center) between two adjacent pores will be constant when using a determinate anodize voltage and acid solution, which is about 100 nm (100.4 ± 0.3 nm, under our experiment data) for oxalic acid solution at 40 V. The longer pore-widening duration would obviously increase the pore diameter, and hence largely decrease the interpore distance. However, excess pore-widening treatment would lead to the UTAM collapse when the pore wall is too thin to support. Therefore, appropriately prolonging pore-widening time, a series of UTAMs with increased pore

DOI: 10.1021/acsami.5b01524
ACS Appl. Mater. Interfaces 2015, 7, 13322−13328

diameters and decreased interpore gaps were obtained. The spacing size between two adjacent pores of the UTAMs is equal to the particle center−center spacing (S), as shown in Figure 1d. This pore-widening process for UTAM allows us to tune the pore diameter and hence to flexibly adjust the gap between the neighboring Ag NPs in an array to get the smallest hot-spot size during the subsequent deposition process ($G = S - D$). In this work, the smallest gap size obtained is 5 nm. Besides the UTAM structure parameters, the size, density, and shape of Ag NPs are dependent on the value of Ag deposition thickness and evaporation rate. To obtain uniform, controllable, hemispherical, and well-aligned Ag NPs in the UTAM pores, the appropriate evaporation rate and nominal layer thickness were about 0.4 nm s^{-1} and 50 nm, respectively.

SEM images of UTAMs with different pore diameters are shown in Figure 2a−f. As can be seen from these images,

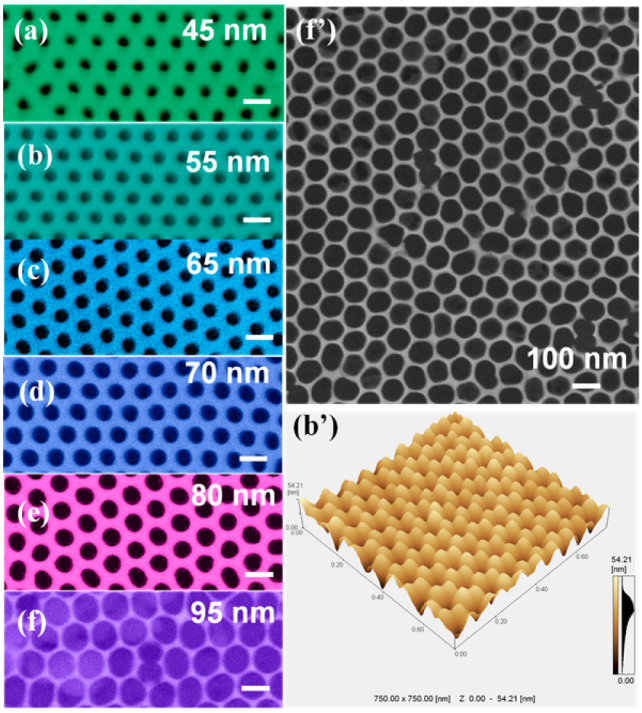

Figure 2. Top-view SEM images of the UTAMs with different pore diameters of (a) 45 nm, (b) 55 nm, (c) 65 nm, (d) 70 nm, (e) 80 nm, (f) and 95 nm. (f′) SEM image of large area UTAM with the pore diameter of 95 nm and (b′) AFM image corresponding to part b. All scale bars are 100 nm.

nanochannel arrays with hexagonal periodicity are highly uniform, and hence, high uniformities of ordered Ag NP arrays over large area (>1 cm^2) are obtained easily through controlling the structure parameters of UTAMs. With the average pore size of UTAMs increased from 45 to 95 nm, the according interpore distance decreases from 55 to 5 nm (obtained by measuring 150 pores for every sample with ImageJ software). The biggest pore diameter of UTAMs in our experiment is about 95 nm (seen in Figure 2f) in the pore-widening process. Figure 2b′,f′ reveals the high regularity and uniformity of large area UTAMs with 55 and 95 nm pore diameter.

Ag NP array SERS-active substrates were obtained using the above UTAMs as templates. The top-view SEM images (Figure 3a−f) of typical Ag NP arrays with different diameters and interparticle gaps and the corresponding SERS properties

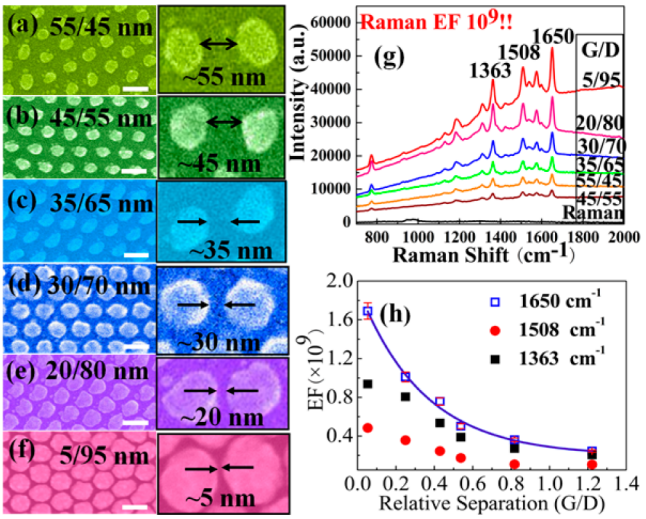

Figure 3. (a−f) SEM images of the typical Ag NP arrays with different diameters and interparticle gaps (G/D) and (g, h) the corresponding SERS properties. (g) SERS spectra of 10^{-7} M R6G molecules on the AgNP arrays substrates with G/D of 55/45, 45/55, 35/65, 30/70, 20/80, and 5/95, and the normal Raman signal of 0.2 M R6G on bare Si substrate. (h) EFs recorded as a function of the relative separation (G/D). The exponential growth fitting curve formula of dependence of EF on G/D at 1650 cm^{-1} peak is $EF = 0.196 + 1.742 \times \exp^{((G/D)/(-0.341))}$. The fitting errors are 0.060, 0.075, and 0.039, respectively. The correlation coefficient, r^2, is 0.995. The original fitting results (including 1508 and 1363 cm^{-1} peaks) are shown in Supporting Information Figure S2. All scale bars are 100 nm. It should be noted that there are smaller nanoparticles around the bigger particles (a−e), which should play a very limited role in SERS activities. These smaller nanoparticles can be avoided by using a strong adhesive tape to peel off the UTAM after Ag deposition. During the Ag deposition, a key issue is keeping low deposition rates (normally we keep 0.2−0.4 nm/s), because a high deposition rate is easy to form big clusters on the top of the UTAM which can block the nanoholes in UTAM.

(Figure 3g,h) are shown in Figure 3. As illustrated in Figure 3a−f, the ordered Ag NP arrays are hexagonally close packed which is a replica of the UTAM nanopores. With the average diameter of Ag NPs increasing from 45 to 55, 65, 70, 80, and 95 nm, the corresponding average interparticle gap decreases from 55 to 45, 35, 30, 20, and 5 nm (inset shows), respectively. Therefore, the gap size between adjacent nanoparticles was tunable to suit a SERS-active substrate by controlling the pore diameter of UTAMs. To understand the dependence of SERS-activity on interparticle gap for the NP arrays, the SERS performances of aqueous R6G solution for various Ag NP arrays were measured using a 514.5 nm argon ion laser and displayed in Figure 3g,h. Figure 3g shows the collection of SERS spectra of R6G (1×10^{-7} M) adsorbed on the Ag NPs samples with gap size of 55, 45, 35, 30, 20, 5 nm and the normal Raman signal of R6G (0.2 M) on bare Si substrate sample. It can be seen that the normal Raman spectrum reveals a very weak Raman signal which cannot provide meaningful structural information on R6G. Interestingly, the SERS spectra of 1×10^{-7} M R6G on Ag NPs obviously show the characteristic signal of R6G. The band at 770 cm^{-1} is assigned to C−H out-of-plane bending mode, and the bands at 1311 and 1575 cm^{-1} are assigned to the N−H in-plane bending modes. The more pronounced bands at 1363, 1508, and 1650 cm^{-1} can be assigned to the aromatic C−C stretching vibrations.[49−51] As expected, SERS peak intensity increases with the decrease of

DOI: 10.1021/acsami.5b01524
ACS Appl. Mater. Interfaces 2015, 7, 13322−13328

the Ag NP separation. With the G value of inter-Ag NP decreasing from 55 to 5 nm, the SERS intensity increased almost 6 times for 1650 cm^{-1} peak (Figure 3g). In a comparison of the SERS signal on the Ag film of the same 50-nm-thick evaporated on Si wafer, the peak intensity increased from nearly 4 times to more than 20 times as the G size decreased from 55 to 5 nm for 1650 cm^{-1} peak, as shown in Supporting Information Figure S1.

In order to quantitatively study the SERS enhancement ability for the substrates, the substrate average enhanced factors for 10^{-7} M R6G molecules on the samples with different Ag NPs separations were estimated according to the equation EF = $(I_{SERS}/I_{NR})(C_{NR}/C_{SERS})$.[49,52−56] (More details are shown in Supporting Information.) The calculated EFs at three main peaks of 1363, 1508, and 1650 cm^{-1} are shown in Supporting Information Table S1. EFs increase obviously with the interparticle gap decreasing from 55 to 5 nm, be higher than 10^9 as the G decreasing to 20 nm, and the highest EF (1.69×10^9) occurred at the smallest G, 5 nm. To visually understand the dependence of EF on the G, EFs of the three main peaks as a function of the relative separation (the ratio of interparticle gap to diameter, G/D) are studied, shown in Figure 3h. For 1363, 1508, and 1650 cm^{-1} peaks, EFs show the same exponentially growth trends with the decreasing G/D, and the fastest growth occurred at 1650 cm^{-1} band. The exponential growth fitting curve formula of dependence of EF on G/D at 1650 cm^{-1} is EF = $0.196 + 1.742 \times \exp^{((G/D)/(-0.341))}$. The same fitting procedure for the other two Raman bands (1508 and 1363 cm^{-1}) is shown in Supporting Information.

The high enhancements are due to the extremely high density of both Ag NPs ($\sim 10^{10}-10^{12}$ cm^{-2}) and small "hot spots" ($\sim 3 \times 10^{10}-10^{12}$ cm^{-2}) on SERS substrates and hence the strong plasmonic coupling between the adjacent Ag NP pairs[57]with sub-10-nm (especially 5 nm) nanogaps, where the electromagnetic field can be amplified dramatically. So, the SERS EF increases remarkably. This demonstrated the sensitive SERS activity for the 5-nm-gap substrate.

The local EM fields of all samples were calculated using an FDTD method (details in the Supporting Information) to further study the dependence of Raman signal enhancement on the NP diameter and interparticle gap. The simulated geometry corresponded to the large 2D array of silver NPs on the Si wafer substrate which is approximated by hexagonally arranged hemispheres with different dimensional parameters (D, G, shown as Supporting Information Figure S3) equal to the mean values of the samples produced experimentally. In the color scale of the EM-field distributions shown in Figure 3, one can find that the field strengths depend significantly on the hemisphere sizes as well as the gaps between them. The largest enhancement is achieved at the smallest 5 nm gap (hot spot). The simulation is in agreement with our experiments.

Although many different SERS substrates have been reported in the literature, one of the problems that still remain is the large-scale homogeneity and reproducibility in Raman enhancement spectra. The advantages of our method for SERS substrate fabrication by UTAM are that we can easily tune and precisely control the interparticle gap even below several nanometers without any loss of the structural uniformity, which ensured the reproducibility of SERS signals. To illustrate the homogeneity of the prepared NP array substrate and reproducibility of the SERS signal, Raman mapping (Figure 4a) was taken on an area of 20×20 μm^2 and SERS spectra (Figure 4c), taken from 10 different sites chosen randomly on

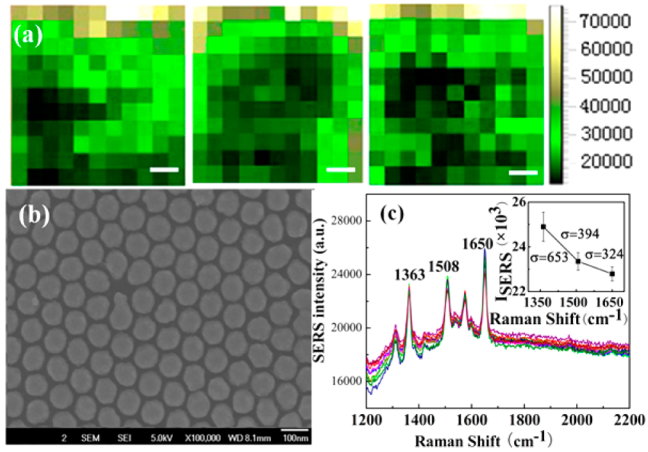

Figure 4. (a) Selected SERS maps of Rhodamine 6G molecules (1600−1700 cm^{-1}, 20×20 μm^2, step size 2 μm) on the 5-nm-gap Ag NPs substrate with the average intensities integrated, scale bar: 4 μm. (b) A typical SEM image of the AgNP array over a large area. (c) Spectra measured at 10 different regions on a 1 cm^2 area of 5-nm-gap Ag NP array show that variation in the SERS spectra was about 2%. The inset shows the standard deviation and the average value of the three prominent peaks at 1363, 1508, and 1650 cm^{-1}. All scale bars are 4 μm.

an entire 1 cm^2 area for the G-5 sample (the sample with the highest SERS enhancement) for 10^{-7} M R6G. Figure 4a displays three of the spot-to-spot SERS maps for different areas (20×20 μm^2) of the substrate, which were recorded with a step of 2 μm using the integrated area of the baseline-corrected peaks at 1650 cm^{-1}. The color distribution shows that the SERS signal intensities tend to be uniform. Moreover, the average intensities of SERS mapping obtained from the intensity distribution resulting from three different areas of the substrate are very close, indicating that the fabricated Ag NPs substrates are uniform and have highly reproducible SERS performance. The low magnification SEM image (shown in Figure 4b) of the Ag NPs arrays (G = 5 nm) revealed ordered NP arrays on a large area SERS substrate which possesses high spatial homogeneity without noticeable defects over a relatively large area. For the spectra of 10 random locations in the sample there are no changes in the characteristic peaks of the spectra except for very minimal variations in the intensity at various points, as shown in Figure 4c. In order to further explain the high reproducibility of the substrate, RSDs in SERS intensity at three prominent peaks at 1363, 1508, and 1650 cm^{-1} (2.62%, 1.69%, and 1.41%, respectively) for 10^{-7} M R6G on the G-5 nm substrate were calculated and shown in Figure 4c, inset. The RSDs as low as 1−3% reveal excellent uniformity of the as-prepared substrate with 5 nm gap. Although less than 20% variation in SERS intensity between various points of the substrate is very acceptable for SERS quantitative studies,[40] there is always a high demand for better reproducibility and more stable SERS substrates. In a comparison with the previously reported substrates with RSD less than 5−10%[9,42,58] or even in the range 2−3% on an area of about 1 mm,[3,45] our observed SERS intensity variation (about 2%) with high enhancement in such a large area (>1 cm^2) is probably the smallest. Apparently, the well-ordered distribution of hot spots endows the substrate with high reproducibility.[6] Moreover, the high density ($\sim 3 \times 10^{10}-10^{12}$ cm^{-2}) of the hot spots (nanogaps about 5 nm) is greatly beneficial to obtain a uniform SERS signal.[59,60]With lower concentration of the

DOI: 10.1021/acsami.5b01524
ACS Appl. Mater. Interfaces 2015, 7, 13322−13328

probe molecule, particularly at the ultralow concentration, better reproducibility can be expected.[60] The low value of RSD and the high EF of SERS signals indicate the as-prepared substrate may be promising for highly sensitive and uniform SERS detection, which demonstrates the most important advantage of the UTAM surface pattern technique.

The minimum gap is 5 nm in the present experiments of this paper, and smaller gaps than 5 nm are goals for fabrication to get better SERS performance. Moreover, so far all the UTAMs that were utilized in the experiments are conventional templates with a limited range of pore arrangement regularity. Recently, UTAM templates with regular pores on millimeter-sized pore regularity have been prepared successfully in our work.[61] This kind of long-range regular template could also be used to fabricate similar Ag nanoparticle arrays with much higher regularity in a larger area, resulting in even higher EF, excellent spatial homogeneity, and highly controllable SERS performance.

4. CONCLUSIONS

In summary, the preparation of highly enhanced and reproducible SERS substrates of Ag NP arrays with very small gaps (~5 nm) is demonstrated on the basis of a UTAM technique. The very high EF (as high as 10^9) and the excellent reproducibility (~1−3% RSD in an entire area of 1 cm^2) of the SERS signal are obtained, which demonstrate the advantages of the well-defined nanogap substrate with high structure tunability and SERS performance controllability on a large area, inexpensive, and easily controllable fabrication method. FDTD calculations further indicate that the excellent SERS characteristics are due to the high density and abundance of very small (about 5 nm or smaller) hot spots. The Ag NP arrays show great potential for the development of sensitive, cost-effective, and large area SERS-based sensors. With further control of the patterning process, it is possible to realize nanopatterns with even smaller spacing than 5 nm, so higher SERS EF is anticipated.

■ ASSOCIATED CONTENT

Supporting Information

Fabrication of UTAMs and ordered Ag nanoparticle arrays, EF calculation, and FDTD simulation results. The Supporting Information is available free of charge on the ACS Publications website at DOI: 10.1021/acsami.5b01524.

■ AUTHOR INFORMATION

Corresponding Authors

*E-mail: mhwu@shu.edu.cn.

*E-mail: leiyong@shu.edu.cn; yong.lei@tu-ilmenau.de.

Author Contributions

Q.F. and Z.Z. contributed equally.

Notes

The authors declare no competing financial interest.

■ ACKNOWLEDGMENTS

This work was supported by Program for Innovative Research Team in University (No. IRT13078), National Science Foundation of China (51301104), Shanghai Thousand Talent Plan, and European Research Council (Three D surface: 240144), BMBF (ZIK-3DNanoDevice: 03Z1MN11), and BMBF (Meta-ZIK-BioLithoMorphie: 03Z1M511) in Germany.

■ REFERENCES

(1) Nie, S. M.; Emery, S. R. Probing Single Molecules and Single Nanoparticles by Surface-Enhanced Raman Scattering. *Science* **1997**, *275*, 1102−1106.

(2) Kneipp, K.; Wang, Y.; Kneipp, H.; Perelman, L. T.; Itzkan, I.; Dasari, R. R.; Feld, M. S. Single Molecule Detection Using Surface-Enhanced Raman Scattering (SERS). *Phys. Rev. Lett.* **1997**, *78*, 1667−1670.

(3) Fleischmann, M.; Hendra, P. J.; McQuilla, Aj. Raman-Spectra of Pyridine Adsorbed at a Silver Electrode. *Chem. Phys. Lett.* **1974**, *26*, 163−166.

(4) Jeanmaire, D. L.; Vanduyne, R. P. Surface Raman Spectroelectrochemistry 0.1. Heterocyclic, Aromatic, and Aliphatic-Amines Adsorbed on Anodized Silver Electrode. *J. Electroanal. Chem.* **1977**, *84*, 1−20.

(5) Qiu, T.; Zhang, W. J.; Lang, X. Z.; Zhou, Y. J.; Cui, T. J.; Chu, P. K. Controlled Assembly of Highly Raman-Enhancing Silver Nanocap Arrays Templated by Porous Anodic Alumina Membranes. *Small* **2009**, *5*, 2333−2337.

(6) Liu, X.; Shao, Y.; Tang, Y.; Yao, K. F. Highly Uniform and Reproducible Surface Enhanced Raman Scattering on Air-stable Metallic Glassy Nanowire Array. *Sci. Rep.* **2014**, *4*, 5835.

(7) Osinkina, L.; Lohmueller, T.; Jaeckel, F.; Feldmann, J. Synthesis of Gold Nanostar Arrays as Reliable, Large-Scale, Homogeneous Substrates for Surface-Enhanced Raman Scattering Imaging and Spectroscopy. *J. Phys. Chem. C* **2013**, *117*, 22198−22202.

(8) Sanchez-Gaytan, B. L.; Swanglap, P.; Lamkin, T. J.; Hickey, R. J.; Fakhraai, Z.; Link, S.; Park, S. J. Spiky Gold Nanoshells: Synthesis and Enhanced Scattering Properties. *J. Phys. Chem. C* **2012**, *116*, 10318−10324.

(9) Barmi, M. R.; Andreou, C.; Hoonejani, M. R.; Moskovits, M.; Meinhart, C. D. Aggregation Kinetics of SERS-Active Nanoparticles in Thermally Stirred Sessile Droplets. *Langmuir* **2013**, *29*, 13614−13623.

(10) Santoro, G.; Yu, S.; Schwartzkopf, M.; Zhang, P.; Vayalil, S. K.; Risch, J. F. H.; Rübhausen, M. A.; Hernández, M.; Domingo, C.; Roth, S. V. Silver Substrates for Surface Enhanced Raman Scattering: Correlation between Nanostructure and Raman Scattering Enhancement. *Appl. Phys. Lett.* **2014**, *104*, 243107.

(11) Liberman, V.; Yilmaz, C.; Bloomstein, T. M.; Somu, S.; Echegoyen, Y.; Busnaina, A.; Cann, S. G.; Krohn, K. E.; Marchant, M. F.; Rothschild, M. A Nanoparticle Convective Directed Assembly Process for the Fabrication of Periodic Surface Enhanced Raman Spectroscopy Substrates. *Adv. Mater.* **2010**, *22*, 4298−4302.

(12) Fan, J. A.; Wu, C. H.; Bao, K.; Bao, J. M.; Bardhan, R.; Halas, N. J.; Manoharan, V. N.; Nordlander, P.; Shvets, G.; Capasso, F. Self-Assembled Plasmonic Nanoparticle Clusters. *Science* **2010**, *328*, 1135−1138.

(13) Theiss, J.; Pavaskar, P.; Echternach, P. M.; Muller, R. E.; Cronin, S. B. Plasmonic Nanoparticle Arrays with Nanometer Separation for High-Performance SERS Substrates. *Nano Lett.* **2010**, *10*, 2749−2754.

(14) Slaughter, L. S.; Wu, Y.; Willingham, B. A.; Nordlander, P.; Link, S. Effects of Symmetry Breaking and Conductive Contact on the Plasmon Coupling in Gold Nanorod Dimers. *ACS Nano* **2010**, *4*, 4657−4666.

(15) Yokota, Y.; Ueno, K.; Misawa, H. Essential Nanogap Effects on Surface-Enhanced Raman Scattering Signals from Closely Spaced Gold Nanoparticles. *Chem. Commun.* **2011**, *47*, 3505−3507.

(16) Ueno, K.; Juodkazis, S.; Mizeikis, V.; Sasaki, K.; Misawa, H. Clusters of Closely Spaced Gold Nanoparticles as a Source of Two-Photon Photoluminescence at Visible Wavelengths. *Adv. Mater.* **2008**, *20*, 26−30.

(17) Duan, H. G.; Hu, H. L.; Kumar, K.; Shen, Z. X.; Yang, J. K. W. Direct and Reliable Patterning of Plasmonic Nanostructures with Sub-10-nm Gaps. *ACS Nano* **2011**, *5*, 7593−7600.

(18) Haynes, C. L.; Van Duyne, R. P. Nanosphere Lithography: A Versatile Nanofabrication Tool for Studies of Size-Dependent Nanoparticle Optics. *J. Phys. Chem. B* **2001**, *105*, 5599−5611.

DOI: 10.1021/acsami.5b01524
ACS Appl. Mater. Interfaces 2015, 7, 13322−13328

(19) Lesuffleur, A.; Kumar, L. K. S.; Brolo, A. G.; Kavanagh, K. L.; Gordon, R. Apex-enhanced Raman Spectroscopy Using Double-Hole Arrays in a Gold Film. *J. Phys. Chem. C* **2007**, *111*, 2347−2350.
(20) Amarandei, G.; O'Dwyer, C.; Arshak, A.; Corcoran, D. Fractal Patterning of Nanoparticles on Polymer Films and Their SERS Capabilities. *ACS Appl. Mater. Interfaces* **2013**, *5*, 8655−8662.
(21) Goldberg-Oppenheimer, P.; Mahajan, S.; Steiner, U. Hierarchical Electrohydrodynamic Structures for Surface-Enhanced Raman Scattering. *Adv. Mater.* **2012**, *24*, OP175−OP180.
(22) Liu, H. M.; Zhang, X. P.; Zhai, T. R.; Sander, T.; Chen, L. M.; Klar, P. J. Centimeter-Scale-Homogeneous SERS Substrates With Seven-Order Global Enhancement Through Thermally Controlled Plasmonic Nanostructures. *Nanoscale* **2014**, *6*, 5099−5105.
(23) Ward, D. R.; Huser, F.; Pauly, F.; Cuevas, J. C.; Natelson, D. Optical Rectification and Field Enhancement in a Plasmonic Nanogap. *Nat. Nanotechnol.* **2010**, *5*, 732−736.
(24) Ward, D. R.; Grady, N. K.; Levin, C. S.; Halas, N. J.; Wu, Y. P.; Nordlander, P.; Natelson, D. Electromigrated Nanoscale Gaps for Surface-Enhanced Raman Spectroscopy. *Nano Lett.* **2007**, *7*, 1396−1400.
(25) Liu, M. N.; Sun, L.; Cheng, C. W.; Hu, H. L.; Shen, Z. X.; Fan, H. J. Highly Effective SERS Substrates Based on An Atomic-Layer-Depositiontailored Nanorod ArrayScaffold. *Nanoscale* **2011**, *3*, 3627−3630.
(26) Im, H.; Bantz, K. C.; Lindquist, N. C.; Haynes, C. L.; Oh, S. H. Vertically Oriented Sub-10-nm Plasmonic Nanogap Arrays. *Nano Lett.* **2010**, *10*, 2231−2236.
(27) Qin, L. D.; Park, S.; Huang, L.; Mirkin, C. A. On-Wire Lithography. *Science* **2005**, *309*, 113−115.
(28) Chen, X. D.; Yeganeh, S.; Qin, L. D.; Li, S. Z.; Xue, C.; Braunschweig, A. B.; Schatz, G. C.; Ratner, M. A.; Mirkin, C. A. Chemical Fabrication of Heterometallic Nanogaps for Molecular Transport Junctions. *Nano Lett.* **2009**, *9*, 3974−3979.
(29) Braunschweig, A. B.; Schmucker, A. L.; Wei, W. D.; Mirkin, C. A. Nanostructures Enabled by On-Wire Lithography (OWL). *Chem. Phys. Lett.* **2010**, *486*, 89−98.
(30) Osberg, K. D.; Schmucker, A. L.; Senesi, A. J.; Mirkin, C. A. One-Dimensional Nanorod Arrays: Independent Control of Composition, Length, and Interparticle Spacing with Nanometer Precision. *Nano Lett.* **2011**, *11*, 820−824.
(31) Osberg, K. D.; Rycenga, M.; Harris, N.; Schmucker, A. L.; Langille, M. R.; Schatz, G. C.; Mirkin, C. A. Dispersible Gold Nanorod Dimers with Sub-5 nm Gaps as Local Amplifiers for Surface-Enhanced Raman Scattering. *Nano Lett.* **2012**, *12*, 3828−3832.
(32) Chen, Z.; Lei, Y.; Chew, H. G.; Teo, L. W.; Choi, W. K.; Chim, W. K. Synthesis of Germanium Nanodots on Silicon Using an Anodic Alumina Membrane Mask. *J. Cryst. Growth* **2004**, *268*, 560−563.
(33) Yang, S. K.; Lei, Y. Recent Progress on Surface Pattern Fabrications Based on Monolayer Colloidal Crystal Templates and Related Applications. *Nanoscale* **2011**, *3*, 2768−2782.
(34) Lei, Y.; Liang, C. H.; Wu, Y. C.; Zhang, L. D.; Mao, Y. Q. Preparation of Highly Ordered Nanoporous Co Membranes Assembled by Small Quantum-Sized Co Particles. *J. Vac. Sci. Technol., B: Microelectron. Nanometer Struct.—Process., Meas., Phenom.* **2001**, *19*, 1109−1114.
(35) Lei, Y.; Yang, S.; Wu, M.; Wilde, G. Surface Patterning Using Templates: Concept, Properties and Device Applications. *Chem. Soc. Rev.* **2011**, *40*, 1247−1258.
(36) Lei, Y.; Cai, W.; Wilde, G. Highly Ordered Nanostructures With Tunable Size, Shape and Properties: A New Way to Surface Nano-Patterning Using Ultra-Thin Alumina Masks. *Prog. Mater. Sci.* **2007**, *52*, 465−539.
(37) Wu, M.; Wen, L.; Lei, Y.; Ostendorp, S.; Chen, K.; Wilde, G. Ultrathin Alumina Membranes for Surface Nanopatterning in Fabricating Quantum-Sized Nanodots. *Small* **2010**, *6*, 695−699.
(38) Zheng, Y.; Wang, W.; Fu, Q.; Wu, M.; Shayan, K.; Wong, K. M.; Singh, S.; Schober, A.; Schaaf, P.; Lei, Y. Surface-Enhanced Raman Scattering (SERS) Substrate Based on Large-Area Well-Defined Gold Nanoparticle Arrays with High SERS Uniformity and Stability. *ChemPlusChem* **2014**, *79*, 1622−1630.
(39) Fu, Q.; Wong, K. M.; Zhou, Y.; Wu, M. H.; Lei, Y. Ni/Au Hybrid Nanoparticle Arrays as A Highly Efficient, Cost-Effective and Stable SERS Substrate. *RSC Adv.* **2015**, *5*, 6172−6180.
(40) Luo, Z. X.; Yang, W. S.; Peng, A. D.; Ma, Y.; Fu, H. B.; Yao, J. N. Net-like Assembly of Au Nanoparticles as a Highly Active Substrate for Surface-Enhanced Raman and Infrared Spectroscopy. *J. Phys. Chem. A* **2009**, *113*, 2467−2472.
(41) Lee, S. J.; Guan, Z. Q.; Xu, H. X.; Moskovits, M. Surface-Enhanced RamanSpectroscopy and Nanogeometry: The Plasmonic Origin of SERS. *J. Phys. Chem. C* **2007**, *111*, 17985−17988.
(42) Wang, H. H.; Liu, C. Y.; Wu, S. B.; Liu, N. W.; Peng, C. Y.; Chan, T. H.; Hsu, C. F.; Wang, J. K.; Wang, Y. L. Highly Raman-Enhancing Substrates Based on Silver Nanoparticle Arrays with Tunable Sub-10 nm Gaps. *Adv. Mater.* **2006**, *18*, 491−495.
(43) Lee, S. J.; Morrill, A. R.; Moskovits, M. Hot Spots in Silver Nanowire Bundles for Surface-Enhanced Raman Spectroscopy. *J. Am. Chem. Soc.* **2006**, *128*, 2200−2201.
(44) Terekhov, S. N.; Mojzes, P.; Kachan, S. M.; Mukhurov, N. I.; Zhvavyi, S. P.; Panarin, A. Y.; Khodasevich, I. A.; Orlovich, V. A.; Thorel, A.; Grillon, F.; Turpin, P. Y. A Comparative Study of Surface-Enhanced Raman Scattering from Silver-Coated Anodic Aluminum Oxide and Porous Silicon. *J. Raman Spectrosc.* **2011**, *42*, 12−20.
(45) Dinish, U. S.; Yaw, F. C.; Agarwal, A.; Olivo, M. Development of Highly Reproducible Nanogap SERS Substrates: Comparative Performance Analysis and Its Application for Glucose Sensing. *Biosens. Bioelectron.* **2011**, *26*, 1987−1992.
(46) Ameer, F. S.; Pittman, C. U., Jr.; Zhang, D. Quantification of Resonance Raman Enhancement Factors for Rhodamine 6G (R6G) in Water and on Gold and Silver Nanoparticles: Implications for Single-Molecule R6G SERS. *J. Phys. Chem. C* **2013**, *117*, 27096−27104.
(47) Zrimsek, A. B.; Henry, A.-I.; Van Duyne, R. P. Single Molecule Surface-Enhanced Raman Spectroscopy without Nanogaps. *J. Phys. Chem. Lett.* **2013**, *4*, 3206−3210.
(48) Lei, Y.; Chim, W. K.; Zhang, Z. P.; Zhou, T. J.; Zhang, L. D.; Meng, G. W.; Phillipp, F. Ordered Nanoporous Nickel Films and Their Magnetic Properties. *Chem. Phys. Lett.* **2003**, *380*, 313−318.
(49) Habouti, S.; Mátéfi-Tempfli, M.; Solterbeck, C.-H.; Es-Souni, M.; Mátéfi-Tempfli, S.; Es-Souni, M. On-Substrate, Self-Standing Au-Nanorod Arrays Showing Morphology Controlled Properties. *Nano Today* **2011**, *6*, 12−19.
(50) Lu, Y.; Liu, G. L.; Lee, L. P. High-Density Silver Nanoparticle Film with Temperature-Controllable Interparticle Spacing for a Tunable Surface Enhanced Raman Scattering Substrate. *Nano Lett.* **2005**, *5*, 5−9.
(51) Liu, M.; Sun, L.; Cheng, C.; Hu, H.; Shen, Z.; Fan, H. J. Highly Effective SERS Substrates Based on an Atomic-layer-depositiontailored Nanorod Array Scaffold. *Nanoscale* **2011**, *3*, 3627−3630.
(52) Le Ru, E. C.; Blackie, E.; Meyer, M.; Etchegoin, P. G. Surface Enhanced Raman Scattering Enhancement Factors: A Comprehensive Study. *J. Phys. Chem. C* **2007**, *111*, 13794−13803.
(53) Choi, D.; Choi, Y.; Hong, S.; Kang, T.; Lee, L. P. Self-Organized Hexagonal-Nanopore SERS Array. *Small* **2010**, *6*, 1741−1744.
(54) Zhang, X.; Zhu, Y.; Yang, X.; Zhou, Y.; Yao, Y.; Li, C. Multifunctional Fe_3O_4@TiO_2@Au Magnetic Microspheres as Recyclable Substrates for Surface-enhanced Raman Scattering. *Nanoscale* **2014**, *6*, 5971−5979.
(55) Shen, J.; Zhu, Y.; Yang, X.; Zong, J.; Li, C. Multifunctional Fe_3O_4@Ag/SiO_2/Au Core-Shell Microspheres as a Novel SERS-Activity Label via Long-Range Plasmon Coupling. *Langmuir* **2013**, *29*, 690−695.
(56) Yang, X.; Zhong, H.; Zhu, Y.; Shen, J.; Li, C. Ultrasensitive and Recyclable SERS Substrate Based on Au-decorated Si Nanowire Arrays. *Dalton Trans.* **2013**, *42*, 14324−14330.
(57) Halas, N. J.; Lal, S.; Chang, W. S.; Link, S.; Nordlander, P. Plasmons in Strongly Coupled Metallic Nanostructures. *Chem. Rev.* **2011**, *111*, 3913−3961.

DOI: 10.1021/acsami.5b01524
ACS Appl. Mater. Interfaces 2015, 7, 13322−13328

(58) Choi, D.; Choi, Y.; Hong, S.; Kang, T.; Lee, L. P. Self-Organized Hexagonal-Nanopore SERS Array. *Small* **2010**, *6*, 1741−1744.
(59) Schmidt, M. S.; Hubner, J.; Boisen, A. Large Area Fabrication of Leaning Silicon Nanopillars for Surface Enhanced Raman Spectroscopy. *Adv. Mater.* **2012**, *24*, OP11−OP18.
(60) Liu, Z.; Cheng, L.; Zhang, L.; Jing, C.; Shi, X.; Yang, Z. B.; Long, Y. T.; Fang, J. X. Large-Area Fabrication of Highly Reproducible Surface Enhanced Raman Substrate via a Facile Double Sided Tape-Assisted Transfer Approach Using Hollow Au-Ag Alloy Nanourchins. *Nanoscale* **2014**, *6*, 2567−2572.
(61) Zhan, Z. B.; Lei, Y. Sub-100-nm Nanoparticle Arrays with Perfect Ordering and Tunable and Uniform Dimensions Fabricated by Combining Nanoimprinting with Ultrathin Alumina Membrane Technique. *ACS Nano* **2014**, *8*, 3862−3868.

DOI: 10.1021/acsami.5b01524
ACS Appl. Mater. Interfaces 2015, 7, 13322−13328